Available online at www.sciencedirect.com
SCIENCE DIRECT
Thermochimica Acta 443 (2006) 225–230
thermochimica acta
www.elsevier.com/locate/tca

Experimental study on preparation of $LaMO_3$ (M = Fe, Co, Ni) nanocrystals and their catalytic activity

Yanping Wang, Xujie Yang, Lude Lu *, Xin Wang *

Materials Chemistry Laboratory, Nanjing University of Science and Technology, Nanjing 210094, China

Received 24 July 2005; received in revised form 18 January 2006; accepted 29 January 2006

Abstract

The perovskite-type oxides $LaMO_3$ (M = Fe, Co, Ni) were prepared by a glycine combustion method using La $(NO_3)_3{\cdot}6H_2O$ and Fe $(NO_3)_3{\cdot}9H_2O$, Co $(NO_3)_2{\cdot}6H_2O$, Ni $(NO_3)_2{\cdot}6H_2O$ as the raw materials, respectively, and $C_2H_5NO_2$ as gelating agent. The products were characterized by XRD, TEM, HRTEM, SEM and BET. The catalytic activity of $LaMO_3$ (M = Fe, Co, Ni) nanocrystals on thermal decomposition of NH_4ClO_4 (AP) were carried out by DTA and TG. The burning rate of the propellant modified by obtained $LaCoO_3$ was measured by strand burner method. The experimental results showed that the obtained products can play a catalytic role in the thermal decomposition of AP and combustion of AP-based propellant. The order of the catalytic performance of obtained products on AP thermal decomposition is $LaCoO_3 > LaNiO_3 \approx LaFeO_3$. Adding 2% of $LaCoO_3$ nanocrystals to AP decreases the decomposition temperature by 134 °C and increases the heat of decomposition by 0.8 kJ g^{-1}. Compared with basic propellant, the burning rate of propellant modified by 1% $LaCoO_3$ nanocrystals increases around 8%.
© 2006 Elsevier B.V. All rights reserved.

Keywords: Oxides nanocrystals; Glycine method; Catalytic activity; Ammonium perchlorate

1. Introduction

The vast majority of catalysts used in modern chemical industry is based on mixed metal oxides. Among the mixed metal oxides, ABO_3 perovskite-type oxides with A as La, B as transition metal were considered strategic materials due to their prominent electronic, magnetic, optic, catalytic activities and application in many fields [1–4]. Delmastro et al. [5] tested the catalytic activity of $LaFeO_3$ towards combustion of methane, Tiwari et al. and Panneerselvam and Rao [6,7] reported the electrocatalytic activity of $LaCoO_3$ and $LaNiO_3$. The common way to prepare $LaMO_3$ is by solid-state reaction method. This method is very simple, thus this process presents several serious drawbacks, such as high reaction temperature, long preparative temperature and limited degree of chemical homogeneity. In recent years, numerous wet-chemical processes have been performed for preparing finer and more homogeneous $LaMO_3$, such as, co-precipitation method, sol–gel method, etc. [4,8–11].

NH_4ClO_4 (AP) is the most common oxidizer in composite solid propellants. The thermal decomposition characteristics influence the combustion behavior of the propellant [12]. The catalytic activities of some transition metal oxides in the thermal decomposition of AP have been reported [12–14] and improved catalytic performance can be obtained from nanometer-scale catalysts [15–17]. We previously reported the catalytic activities of NiO nanoparticles for the thermal decomposition of AP [18]. While to our knowledge, the perovskite-type oxides have not been reported for this usage. The aim of this work was to investigate the catalytic activities of $LaFeO_3$, $LaCoO_3$ and $LaNiO_3$ nanocrystals prepared by the simple glycine method for the thermal decomposition of AP and the combustion of propellant.

2. Experimental

2.1. Materials

All the reagents were analytical grade chemicals. Co $(NO_3)_2{\cdot}6H_2O$, La $(NO_3)_3{\cdot}6H_2O$ and $C_2H_5NO_2$ were obtained from the Shanghai Chemical Factory; Ni $(NO_3)_2{\cdot}6H_2O$ and Fe $(NO_3)_3{\cdot}9H_2O$ were produced by the Guangdong Xilong chemical factory. Basic propellant containing 5 parts of AL, 60 parts

* Corresponding authors. Tel.: +86 25 84310609; fax: +86 25 84315054.
E-mail address: njwangyp@yahoo.com.cn (L. Lu).

0040-6031/$ – see front matter © 2006 Elsevier B.V. All rights reserved.
doi:10.1016/j.tca.2006.01.030

of AP, 20 parts of RDX(hexahydro-1,3,5-trinitro-1,3,5-triazine) and 15 parts of HTPB(hydroxyl terminated polybutadiene) and other additions was provided by Xi'an North Huian Chemical Industry Limited Company.

2.2. Preparation of $LaMO_3$ (M = Fe, Co, Ni) nanocrystals

$LaMO_3$ (Fe, Co, Ni) nanocrystals were prepared by glycine combustion method. About 10 mmol of each of $La(NO_3)_3 \cdot 6H_2O$ and metal (Fe, Co, Ni) nitrates and 40 mmol of $C_2H_5NO_2$ were dissolved in distilled water in a beaker and the volume of solution was made up to 100 ml. The solutions were continuously magnetic stirring for about 6 h at around 60 °C until sol-like solutions were obtained. The solutions were heated to burning in a self-propagating combustion manner, then the loose as-burnt products were obtained, finally, the powder were sintered at 700 °C for 2 h in air.

2.3. Preparation of samples for catalytic activity experiment

$LaMO_3$ (M = Fe, Co, Ni) nanocrystals and AP were mixed in 2:98 (wt.%) respectively to prepare the samples for the thermal analyses experiment.

The samples for burning rate experiment were prepared by Xi'an North Huian Chemical Industry Limited Company. Basic propellant and besides propellants with 1 part of $LaCoO_3$ nanocrystals added to 100 parts of basic propellant were prepared, totaling to two kinds of samples. Each strand-like sample cut from a block of propellant occupied 4 mm × 4 mm and length 100 mm.

2.4. Instrumentation

X-ray diffraction (XRD) was carried out on a Bruker D8 Advance X-ray diffraction instrument (Cu Kα), the diffraction angle (2θ) from 25° to 80° was scanned. Transmission electron microscopy (TEM) and high-resolution transmission electron microscopy (HRTEM) images were taken with a JEOL JEM-2100 electron microscope; the sample was dispersed in aqueous ethanol by ultrasonic stirring. Scanning electron microscope (SEM) micrographs were taken with a JEOL JSM-6380LV electron microscope. The BET surface areas were measured on a Bechman Coulter SA3100 Plus instrument using N_2 adsorption at −196 °C. Beijing WCT-2A thermal analyzer was used at a heating rate of 20 °C/min in N_2 atmosphere over the range 20–500 °C with Al_2O_3 as reference. The strand burner was employed for each sample at 20 °C, 6 MPa to measure the burning rate.

3. Results and discussion

3.1. Particle characterizations of the obtained products

Fig. 1 shows the XRD spectra of the obtained products. The diffraction date are in agreement with JCPDS card of $LaFeO_3$ (no: 74-2203), $LaCoO_3$ (no: 09-0358) and $LaNiO_3$ (no: 34-1028). The average crystal particle size of obtained products determined from the XRD patterns parameters according to the Scherrer equation [19] are 59, 47 and 14 nm, respectively. The theoretical values of interplanar spacing due to different plane of the obtained products were indicated in Fig. 1.

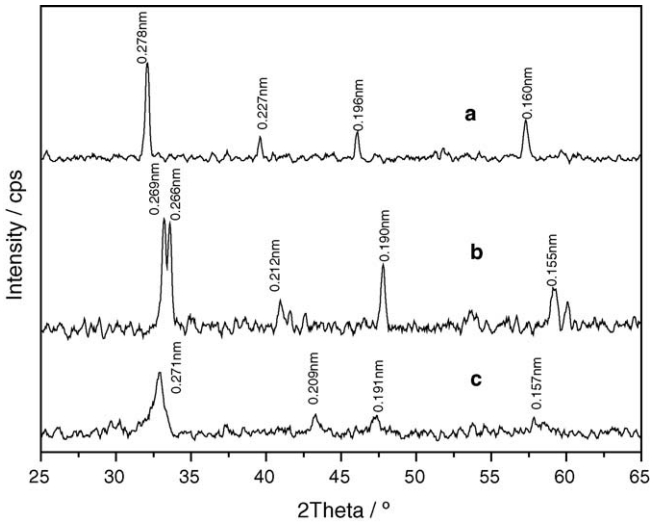

Fig. 1. XRD pattern of: (a) $LaFeO_3$; (b) $LaCoO_3$; (c) $LaNiO_3$.

Fig. 2 displayed the scanning electron micrographs of obtained products. It is seen clearly that each of them is a low density porous material which is favorable to a catalytic application. The BET surface area of $LaMO_3$ (M = Fe, Co, Ni) nanocrystals calculated from N_2 isotherms at −196 °C are 7.6, 8.9 and 7.7 m^2/g, respectively.

In order to measure more precisely particles sizes of these oxides, TEM was used. Typical TEM images (Fig. 3) show that average grain particle size of obtained-products are larger than the crystal grain size primarily due to the presence of agglomerates in the powder.

In Fig. 4, HREM image show the clearly and regularly crystal lattice distance which express highly crystalline $LaMO_3$ (Fe, Co, Ni) were formed having typical crystalline shape. The crystal lattice distance measured from the HRTEM images were 0.28, 0.11 and 0.27 nm, respectively.

3.2. Catalytic effect of the $LaMO_3$ (M = Fe, Co, Ni) on NH_4ClO_4 decomposition

The results of The DTA and TG experiments are shown in Figs. 5 and 6, respectively. The DTA and TG results are also summarized in Table 1.

The DTA curve for neat AP (Fig. 5a) shows three events, while, the TG curve (Fig. 6a) exhibits only two. The first endothermic DTA peak with a peak temperature of 242 °C is accompanied with zero weight loss. This represents the transition from orthorhombic to cubic AP [20]. The first exothermic DTA peak with a peak temperature of 321 °C corresponding 14% weight loss is attributed to the partial decomposition of AP and formation of some intermediate NH_3 and $HClO_4$ by dissociation and sublimation [13,21,22]. The second exothermic DTA peak

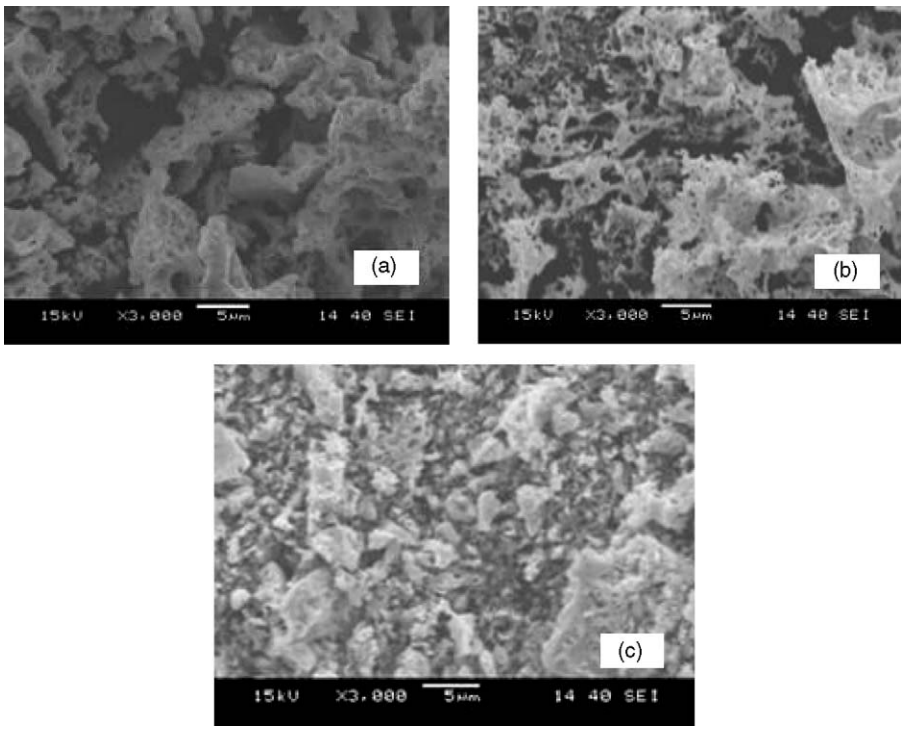

Fig. 2. SEM micrographs of: (a) $LaFeO_3$; (b) $LaCoO_3$; (c) $LaNiO_3$.

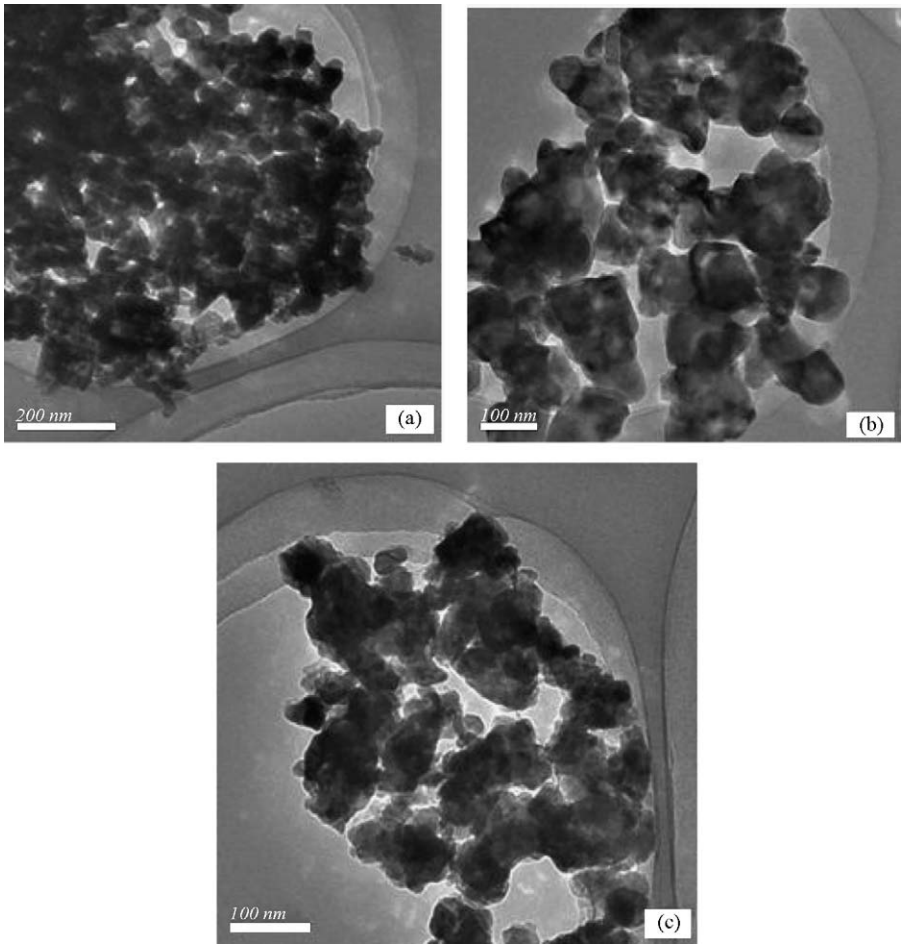

Fig. 3. TEM images of the obtained-products: (a) $LaFeO_3$; (b) $LaCoO_3$; (c) $LaNiO_3$.

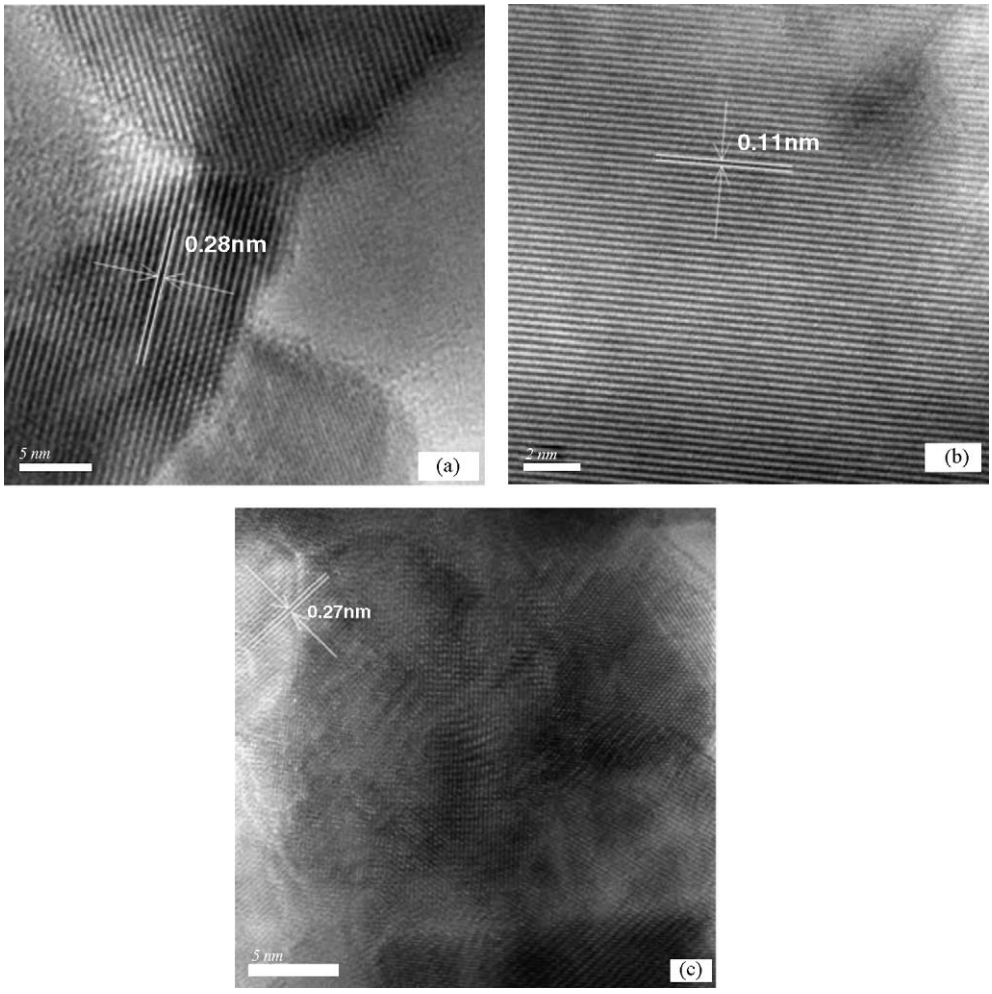

Fig. 4. HRTEM images of the obtained-products: (a) $LaFeO_3$; (b) $LaCoO_3$; (c) $LaNiO_3$.

with a peak temperature of 441 °C associated with 86% weight loss is caused by the complete decomposition of the intermediate to volatile products [13]. The heat of decomposition of neat AP is 0.6 kJ g^{-1}.

As shown in Fig. 5b and d and Fig. 6b and d, the DTA and TG curves for decomposition of AP in presence of $LaFeO_3$ and $LaNiO_3$, respectively, show noticeable changes in the decomposition pattern.

Figs. 5b and 6b are the DTA and TG curves of AP in presence of $LaFeO_3$ catalysts. The peak temperature of first exothermic peak is 317 °C accompanied with ∼35% weight loss and that of second exothermic peak is 374 °C associated with ∼63% weight loss. The decomposition heat of this mixture is 1.0 kJ g^{-1}. Figs. 5d and 6d illustrate the DTA and TG curves of AP in presence of $LaNiO_3$ catalysts. The first exothermic peak temperature appears at 312 °C, related with ∼37% weight loss. The second exothermic peak temperature appears at 377 °C corresponding with ∼61% weight loss. The decomposition heat of this mixture is 1.1 kJ g^{-1}. Based on the above-mentioned results, the first exothermic peaks of these two mixtures are not lower too much than that of neat AP. While, the weight lose of them in first stage are much more than that of neat AP, respectively. Simultaneously, the second exothermic peaks and the second mass loss steps were observed at lower temperature than that of neat AP. These results mean that the both $LaFeO_3$ and $LaNiO_3$ were catalytically active for the thermal decomposition of AP.

Figs. 5c and 6c express the DTA and TG curves of AP in presence of $LaCoO_3$, which show significant changes in the decom-

Table 1
The temperature peak, mass loss, exothermic quantity and phase transition enthalpy of AP and the mixtures

Sample	Phase transition H (J g^{-1})	1st T_p (°C)	1st mass loss (%)	2nd T_p (°C)	2nd mass loss (%)	Total H (exo) (kJ g^{-1})
Neat AP	−87	321	14	441	86	0.6
Ap + $LaFeO_3$	−88	317	35	374	63	1.03
AP + $LaCoO_3$	−86	307	98	–	–	1.42
AP + $LaNiO_3$	−88	312	37	377	61	1.09

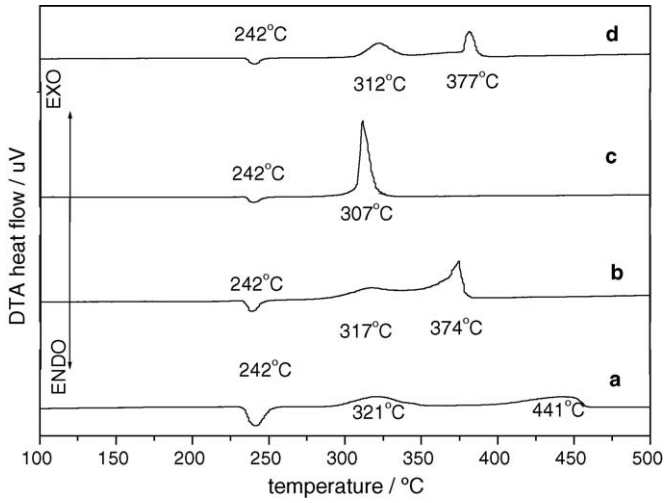

Fig. 5. DTA curves for: (a) neat AP; (b) AP + $LaFeO_3$; (c) AP + $LaCoO_3$; (d) AP + $LaNiO_3$.

position pattern. The first exothermic peak occurs at 307 °C changed into a sharp one associated with only one step weight loss. The second exothermic was absent. The heat of decomposition increases to1.4 kJ g^{-1}. The experiment results indicate that $LaCoO_3$ is obviously a more effective catalyst than $LaFeO_3$ and $LaNiO_3$. The addition of $LaCoO_3$ lowers the decomposition temperature of AP and increases the speed of decomposition and heat of decomposition reaction. AP was completely decomposed in lower temperature and short time.

Moreover, as can be seen in Fig. 6, the onset temperatures of thermal decomposition of the samples are all at about 300 °C, the end temperatures are about at 450, 380, 312 and 375 °C, respectively. So, the speed of thermal decomposition were found to exhibit in an order of AP in presence of $LaCoO_3$ > AP in presence of $LaNiO_3$ ≈ AP in presence of $LaFeO_3$ > neat AP.

The enthalpies of phase transition are all around -87 ± 1 J g^{-1}. The first endothermic peak temperature of AP in presence of catalysts are almost not changed compared with neat AP and no weight loss appear in the phase transition process.

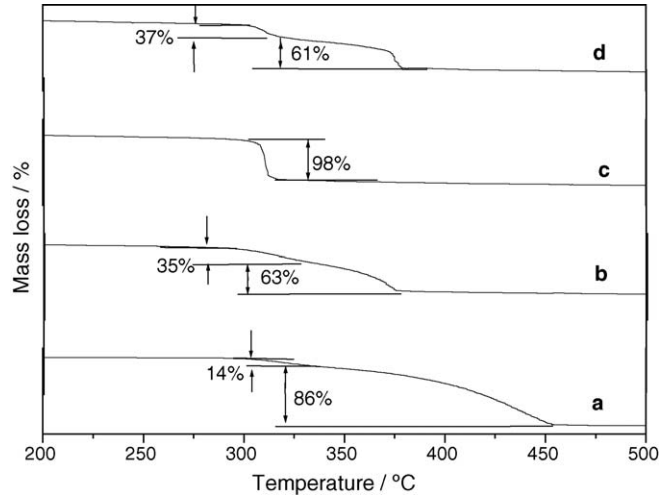

Fig. 6. TG curves for: (a) pure AP; (b) AP + $LaFeO_3$; (c) AP + $LaCoO_3$; (d) AP + $LaNiO_3$.

Table 2
The results of burning rate experiments

Sample	Burning rate (mm/s)					
	1	2	3	4	5	Average
Basic propellants	6.47	6.53	6.58	–	6.48	6.52
Basic propellants + 1%$LaCoO_3$	6.86	7.09	7.00	7.13	7.08	7.01

Hence, the catalysts have no influence on the phase transition of AP.

The detail data of the peak temperature, phase transition enthalpy, enthalpies for decomposition and mass change values of neat AP and the mixture are listed in Table 1

According traditional electron-transfer theory [13], the $LaMO_3$ (M = Fe, Co, Ni) presence of partially filled 3d orbital in M^{3+} and empty 5d orbital in La^{3+} may provide help in electron-transfer process. Positive hole in $LaMO_3$ can accept electrons from perchlorate ion enhancing the thermal decomposition of AP. So, all these three catalysts show catalytic effect on the AP decomposition.

The crystal lattice distance is a parameter relate with energy of crystal and the energy characteristic of catalysts itself effects its catalytic activity. As indicated in Fig. 1, except the crystal lattice distance corresponding 2θ in 41°–43° range, the crystal lattice distances of $LaCoO_3$ are less than that of $LaFeO_3$ and $LaNiO_3$. This may imply that the less crystal lattice distance maybe a reason of more active of $LaCoO_3$. Clearly, however, the further detailed study of the correlation between crystal lattice distance and catalytic activity are necessary.

On the other hand, the catalytic activity is dependent on the specific surface area of the catalyst. The higher specific surface is the better catalytic activity will be. Thus, the more active of $LaCoO_3$ is due to it's relate higher specific surface area which is the second place effect.

3.3. Catalytic effect of $LaCoO_3$ on the burning rate of AP-based propellants

In view of above-mentioned facts, $LaCoO_3$ has been found to be an active catalyst in the thermal decomposition of AP. So, we further investigated the catalytic activity of that on the burning rate of AP-based propellants. The result listed in Table 2 indicates that the addition of $LaCoO_3$ had the effect on burning rate. Adding 1% $LaCoO_3$ nanocrystals to basic propellant, the burning rate of the modified propellant was increased around 8%.

4. Conclusion

$LaMO_3$ (M = Fe, Co, Ni) nanocrystals were synthesized by a simple and fast route. The catalytic activities of obtained-products were experimental study. Combined with the results of thermal decomposition peak temperature, thermal decomposition rate and exothermic quantity, the order of the catalytic effective of $LaMO_3$ (M = Fe, Co, Ni) on thermal decomposition

of AP is $LaCoO_3 > LaNiO_3 \approx LaFeO_3$. In this serial catalyst, the $LaCoO_3$ nanocrystals are best one on the thermal decomposition AP. Adding 2% of $LaCoO_3$ obtained product to AP decreases the decomposition temperature by 134 °C and the heat of decomposition increases by 0.8 kJ g^{-1}. Further burning rate experiment reveals that the $LaCoO_3$ nanocrystals can increase the burning rate of AP-based propellant.

Acknowledgements

The authors are grateful for the financial support of the National Natural Science Foundation of China and National Defense Foundation of China.

References

[1] J.D.G. Fernandes, D.M.A. Melo, L.B. Zinner, C.M. Salustiano, Z.R. Silva, A.E. Martinelli, M. Ceraueira, C. Alves Júnior, E. Longo, M.I.B. Bernardi, Mater. Lett. 53 (2002) 122.
[2] M.A. Peña, J.L.G. Fierro, Chem. Rev. 101 (2001) 1981.
[3] J. Stephen, Skinner, Int. J. Inorg Mater. 3 (2001) 113.
[4] A.K. Norman, M.A. Morris, J. Mater. Process. Tech. 92/93 (1999) 91.
[5] A. Delmastro, D. Mazza, S. Ronchetti, M. Vallino, R. Spinicci, P. Brovetto, M. Salis, Mater. Sci. Eng. B 79 (2001) 140.
[6] S.K. Tiwari, J. Ekoenig, G. Poillerat, P. Chartier, R.N. Singh, J. Appl. Electrochem. 28 (1998) 114.
[7] M. Panneerselvam, K.J. Rao, J. Mater. Chem. 13 (2003) 596.
[8] Y. Zhu, R. Tan, J. Mater. Sci. 35 (2000) 5415.
[9] X. Qi, J. Zhou, Z. Yue, Z. Gui, L. Li., Mater. Chem. Phy. Mater. Sci. Commun. 78 (2002) 25.
[10] W. Zheng, R. Liu, D. Peng, G. Meng, Mater. Lett. 43 (2000) 19.
[11] J. Wang, Q. Liu, D. Xue, F. Li, J. Mater. Sci. Lett. 21 (2002) 1059.
[12] D.V. Survase, M. Gupta, S.N. Asthana, Prog. Cryst. Growth Charact. Mater. (2002) 161.
[13] A.A. Said, R. AI-Qusmi, Thermochim. Acta 275 (1996) 83.
[14] N.B. Singh, A.K. Ojha, Thermochim. Acta 390 (2002) 67.
[15] J. Zhu, H. Chen, B. Xie, X. Yang, L. Lu, X. Wang, Chin. J. Catal. 25 (2004) 637.
[16] J. Zhu, W. Zhang, H. Wang, X. Yang, L. Lu, X. Wang, Chin. J. Inorg. Chem. 20 (2004) 863.
[17] Z. Ma, F. Li, A. Chen, H. Bai, Acta Chim Sin. 13 (2004) 1252.
[18] Y. Wang, J. Zhu, X. Yang, L. Lu, X. Wang, Thermochim. Acta 437 (2005) 106.
[19] X. Liu, X. Wang, J. Zhang, X. Hu, L. Lu, Thermochim. Acta 342 (1999) 67.
[20] T. Ganga Devi, M.P. Kannan, B. Hema, Thermochim. Acta 285 (1996) 269.
[21] W.A. Rosser, S.H. Inami, Combust. Flame 12 (1968) 427.
[22] P.W.M. Jacobsete, Combust. Flame 13 (1969) 419.